The role of $G\alpha_O$-mediated signalling in the rostral ventrolateral medulla oblongata in cardiovascular reflexes and control of cardiac ventricular excitability

Richard Ang, MBBS, MRCP, PhD*‡, Joel Abramowitz PhD#, Lutz Birnbaumer PhD#, Alexander V. Gourine, PhD* and CAAndrew Tinker, MBBS, PhD, FRCP‡

*From the *William Harvey Heart Centre, Barts & The London School of Medicine and Dentistry, London, UK, ‡Department of Neuroscience, Physiology and Pharmacology, University College London, London, UK, #Division of Intramural Research, National Institute of Environmental Health Sciences, 111 T.W. Alexander Dr., Bldg 101, Rm F179 P.O. Box 12233, Mail Drop: F1-10, Research Triangle Park, NC 27709, USA*

CACorresponding author: Andrew Tinker. William Harvey Heart Centre, Barts & The London School of Medicine and Dentistry, London, United Kingdom; Tel +44 20 7882 5783; Fax +44 20 7882 3408; email: a.tinker@qmul.ac.uk

AVG and AT are joint last authors.

Abstract

The heart is controlled by the sympathetic and parasympathetic limbs of the autonomic nervous system with inhibitory signaling mechanisms recruited in both limbs. This study aimed to determine the role of inhibitory heterotrimeric G proteins in the central mechanisms underlying autonomic control of the heart and its potential role in arrhythmogenesis. Mice with conditional deletion of inhibitory heterotrimeric G protein $G\alpha_O$ in the central nervous system (CNS) were generated to determine the effect of specific $G\alpha_O$ deletions on autonomic control and electrophysiological properties of the heart. $G\alpha_O$ deletion in the pre-sympathetic area of the rostral ventral lateral medulla (RVLM) was not associated with changes in heart rate or the arterial blood pressure at rest (home cage, normal behaviour). However, exposure to stressful conditions (novel environment, hypoxia or hypercapnia) in these mice was associated with exaggerated heart rate responses and an increased baroreflex gain when assessed under urethane anaesthesia. This was associated with shortening of the ventricular effective refractory period. This phenotype was reversed following systemic administration of a beta-adrenoceptor blocker atenolol, suggesting that $G\alpha_O$ depletion in the RVLM increases central sympathetic drive. The data obtained suggest that $G\alpha_O$-mediated signalling within the presympathetic circuits of the RVLM contributes to the autonomic control of the heart. $G\alpha_O$ deficiency in the RVLM is associated with exaggerated cardiovascular responses to stress, altered cardiovascular reflexes and electrical properties of the heart.

Key words: G proteins; rostral ventral lateral medulla; blood pressure; cardiac excitability; autonomic nervous system;

Introduction

The heart is controlled by the autonomic nervous system via its two functional limbs: the sympathetic and parasympathetic (35). Sympatho-vagal imbalance can trigger ventricular arrhythmias in patients with inherited 'channelopathies' such as the long QT syndrome, Brugada syndrome and catecholaminergic polymorphic ventricular tachycardia (41) and also in patents with ischemic heart disease (26). Sympathetic denervation has been used as an adjunct to pharmacotherapy with beta-adrenoceptor antagonists in the management of patients with resistant ventricular arrhythmias (40). However, the efficacy of current therapeutic strategies remains limited, perhaps reflecting the fact that only the downstream peripheral mechanisms are targeted.

Heterotrimeric G proteins mediate signalling via G-protein coupled receptors (GPCRs). GPCRs are involved in autonomic control at the level of the heart via beta adrenergic and muscarinic receptors signalling via stimulatory $G\alpha_S$ and inhibitory $G\alpha_{i/o}$ proteins. There appears to be specificity of Gα protein subtypes *in vivo.* Zuberi et al. have demonstrated the importance of the inhibitory G proteins $G\alpha_{i2}$ and $G\alpha_O$ in the autonomic control of the heart using global knockout (KO) mouse models (43). We have recently shown that $G\alpha_{i2}$ is important in mediating parasympathetic influences at the level of the cardiac conduction tissue, probably by coupling to M2 muscarinic receptors (34). What remains unclear is the exact role played by the inhibitory G proteins in the central nervous mechanisms of autonomic regulation of the heart.

$G\alpha_O$ protein is a key inhibitory G protein subtype in the central nervous system (CNS) (36) including the brainstem (28). Mice with global deletion of $G\alpha_O$ are tachycardic and display loss of diurnal rhythm in heart rate and selective loss of the low frequency component of heart rate variability with preserved total power (43). However, carbachol still had a negative chronotropic effect in this model, suggestive of increased sympathetic activity (43). The rostral ventrolateral medulla (RVLM) contains principal pre-sympathetic circuits which generate central sympathetic drive (10,23). Increased activity of the RVLM neurones

has been implicated in the development and progression of cardiovascular diseases associated with enhanced central sympathetic drive including hypertension (21) and heart failure (20). We hypothesized that the inhibitory influences mediated via $G\alpha_O$ proteins in the RVLM are important in controlling (restricting) sympathetic tone. This would broadly impact on blood pressure homeostasis and cardiac function particularly heart rate and ventricular excitability. To test this hypothesis we generated mice with conditional deletion of $G\alpha_O$ in the RVLM and studied their cardiovascular phenotype, cardiovascular reflexes and ventricular excitability *in vivo*.

Methods

Murine husbandry

Mice were maintained in an animal core facility under the UK Home Office guidelines relating to animal welfare. All procedures were approved by the local animal care and use committee and performed in accord with the UK Home Office regulations. All mice were kept in a temperature controlled environment (21-24°C) with 12/12hr light/dark cycle. Animals were allowed ad libitum access to standard rodent chow and drinking water.. Mice were studied between 8-12 weeks of age.

Experimental Animals

$G\alpha_O$ flx/flx mice on a Sv129 background with coding exons 5 to 6 of the $G\alpha_O$ allele on chromosome 8 flanked by loxP sites were generated using homologous recombination in mouse ES cells (39). Gene targeting strategies, genotyping primers and confirmation of selective deletion of $G\alpha_O$ at the protein level from various tissues including the brain using western blot approaches have been previously described (39). Mice with conditional deletion of $G\alpha_O$ in the RVLM were then generated following microinjections of adenoviral vectors (AVV) co-expressing Cre and GFP under the control of a CMV promoter (Cre/GFP-AVV) into the RVLM of $G\alpha_O$ flx/flx mice. Control mice were produced by using GFP-only expressing AVV under the control of the same CMV promoter (GFP-AVV). These vectors have been described previously (13; 14) and were obtained from Viraquest (USA). In preliminary studies, quantitative RT-PCR using TaqMan gene expression assays was performed at sites of injections to confirm knockdown of $G\alpha_O$ expression and determine the optimum dilution of viral titres to be used. Immunohistochemistry was performed at the end of all the experiments to determine co-localisation of GFP expression with tyrosine hydroxylase (TH) immunoreactivity in the RVLM.

Experiments in conscious freely moving mice

Conscious freely behaving $G\alpha_O$ flx/flx mice were first studied in their normal housing conditions and in a plethysmography chamber. Figure 1 illustrates the experimental protocol used.

Biotelemetry recordings of the systemic arterial blood pressure (BP)

BP telemetry probe implantation and recording techniques have been described in detail previously (1). Briefly, the left internal carotid artery was cannulated with a gel-filled catheter of the BP telemetry probe (model PA-C10, Data Sciences International, USA) which allows beat-to-beat biotelemetry recording of the arterial BP in conscious freely moving mouse. Heart rate (HR) was derived from the BP recording trace.

2.5 Recording of the 24 hour BP and HR profile

Animals were allowed to recover for at least 10 days after the transmitter implantation. Experiments were performed in a temperature-controlled environment (21-24°C) with 12hr/12hr light/dark cycle. The animals were allowed to acclimatise to the experimental conditions during the recovery period from surgery. For serial BP and HR measurements, 15 second-long samples were taken every 30 minutes over 24 hours using a 'scheduled sampling' protocol. From the recorded dataset, it was possible to determine the diurnal changes in BP and HR during the day and night and also calculate the mean values.

Whole body plethysmography

Mice with telemetry probes implanted were also exposed to hypoxic and hypercapnic conditions. Respiratory rate (f_R, breaths min^{-1}), tidal volume (V_T, arbitrary unit g^{-1}) and minute ventilation (V_E) ((f_R x V_T); arbitrary unit min^{-1} g^{-1}) were measured using whole body plethysmography as described in detail previously (27; 32; 38) and BP and derived HR simultaneously recorded using radiotelemetry. Briefly, the mouse was placed in a plexiglass recording chamber (~200 ml) that is in turn placed on a telemetry recording mat. The

chamber was flushed continuously with a mixture of 79% nitrogen and 21% oxygen (unless otherwise required by protocol) at a rate of ~1 L min^{-1}. Concentrations of O_2 and CO_2 in the chamber were monitored on-line using a fast-response O_2/CO_2 monitor (Morgan Scientific, USA).

The animals were allowed at least 20 minutes to acclimatise to the chamber environment at normoxia/normocapnia (21% O_2, 79% N_2 and <0.3% CO_2) before measurements of baseline ventilation were taken. Hypoxia was induced by lowering the O_2 concentration in the inspired air down to 10% for 5 minutes. After 5 minutes, the O_2 concentration was then brought back up to 21% for a further 5 minutes. In a separate experiment, normoxic hypercapnia was induced by titrating CO_2 into the respiratory mixture up to a level of 3% or 6% (lowering N_2 accordingly) for 5 minutes at each CO_2 level. The measurements were taken during the last 2 minutes before exposure to the stimulus and during the 2-minute period at the end of each stimulus, when breathing has stabilized. Simultaneous continuous recordings of changes in BP, HR, f_R and V_T during hypoxic and hypercapnic challenges were obtained.

In vivo experiments under general anaesthesia

A separate cohort of $G\alpha_O$ flx/flx mice were studied in the anaesthetized state after Cre/GFP AVV or control GFP AVV injections into the RVLM. Mice were anesthetized with urethane (1.3 g/kg ip). The depth of anesthesia was monitored using the stability of BP, HR and lack of flexor responses to a paw-pinch and supplemental anesthesia was given as required. Body temperature was maintained at 37.0±0.2^{0}C using a servo-controlled heating pad. Tracheostomy was performed to facilitate ventilation in spontaneously breathing mice. Needle electrodes were placed in a lead II configuration to record surface ECG (sampled at 2 kHz, amplified x 50-100 and filtered to a bandwidth between 5 to 100 Hz with 50 Hz notch filtering).

Determining baroreflex sensitivity

The right and left internal jugular veins were cannulated with polyethylene tubing (PE-10) for administration of phenylephrine (0.5-2.5 mg kg^{-1} iv in 2-10 µL saline) or sodium nitroprusside (SNP, 0.1-1 mg kg^{-1} iv in 1-10µL saline), respectively. The left carotid artery was cannulated with saline-filled polyethylene tubing (mechanically stretched PE-10 connected to PE-50) connected to a pressure transducer to measure arterial BP (sampled at 2 kHz). Changes in the systemic arterial BP were induced by alternately administrating phenylephrine and SNP and varying the volumes of injectate. The baroreflex sensitivity curve was then derived as described by Head and McCarty (10). The peak changes in arterial BP and HR were determined following administration of each drug and the changes from basal values were then calculated for each pair of data points and scaled back to absolute BP and HR by the average of all basal values recorded. 10 to 15 data points were obtained across the range of BP-HR for each animal and the data points were then fitted to the following logistic equation using a least squares iterative routine on MatLab (R2010b, MathWorks, MA, USA).

$$\mathbf{HR} = P1 + P2 / [1+e^{P3(\mathbf{BP}-P4)}]$$

where P1 = lower HR plateau, P2 = HR range, P3 = a curvature coefficient which is independent of range and P4 = BP_{50}, i.e. the BP at half the HR range. The average baroreflex gain (BRG) or slope of the curve between the two inflection points is given by BRG = -P2 ×P3/4.56 and the upper plateau = P1 + P2.

Ventricular electrophysiology

A separate group of mice underwent programmed electrical assessment of ventricular excitability. An octapolar 1.1F cardiac electrophysiology catheter was inserted into the right ventricular apex through the right internal jugular vein to pace the heart as previously described (17; 44). Cardiac pacing using extrastimulation protocols was performed with an S88-Grass stimulator to record the ventricular effective refractory period

at a basic drive train of 750 beats per minute ($VERP_{750}$). Finally, a ventricular stimulation protocol was performed by delivering a drive train of 15 S1 beats at increasingly shorter intervals from 80 ms to 20 ms. A successful study was defined as induced V_T that consisted of at least 4 consecutive QRS complexes with different morphology to that recorded in sinus rhythm (8).

Statistical analysis

Data are reported as means ± standard error of the mean (SEM) unless stated otherwise. For determination of statistical significance between groups, 2 tailed Student's *t* test was used for parametric data with a normal distribution and the Mann-Whitney U Test was used as a non-parametric test. Fisher's exact test was used for comparing categorical data. For data with repeated sampling between multiple groups, mixed level modelling using both fixed and random effects was used to compare the mean effect of each group. Analysis of variance with Bonferroni multiple comparison test was used to compare the difference of effect between groups. In all the instances, $P<0.05$ was considered significant.

Results

Generation of mice with conditional deletion of $G\alpha_O$ deletion in the RVLM and controls

Using 1:100 dilutions of Cre/GFP AVV (6 x 10^{10} PFU) and GFP AVV (3 x 10^{10} PFU), $G\alpha_O$ expression at the sites of injections was reduced by 79% in mice post Cre/GFP-AVV injections (relative expression 0.21, 95%CI 0.18-0.25) compared to 21% post GFP-AVV injections (relative expression 0.79, 95%CI 0.75-0.82), when normalized to the expression in mice pre injections (n=3 mice in triplicate for both groups). Figure 2 shows the representative brainstem distribution of GFP expressing cells relative to TH-immunoreactivity.

Diurnal profile of HR and BP changes in conditions of $G\alpha_O$ deletion in the RVLM

We first examined the 24-hour HR and BP profile of $G\alpha_O$ flx/flx mice pre and post Cre/GFP AVV (n=6) and control GFP AVV (n=6) injections under normal housing conditions. There was a clear circadian variation of HR and systolic BP in $G\alpha_O$ flx/flx mice which was unchanged following injections of Cre/GFP AVV and control GFP AVV (Figure 3).

Haemodynamic and respiratory responses to hypoxia and hypercapnia in conditions of $G\alpha_O$ deletion in the RVLM

$G\alpha_O$ flx/flx mice were then studied in the plethysmography chamber. $G\alpha_O$ flx/flx mice responded to hypoxia (10% O_2) with an increase in HR, respiratory rate, tidal volume and minute ventilation, but there was no significant change in the systolic BP. There was post-hypoxic depression of respiratory activity with reduced respiratory rate below baseline and normalisation of HR and tidal volume. In conditions of $G\alpha_O$ deletion in the RVLM (post Cre/GFP AVV injections in $G\alpha_O$ flx/flx mice) the animals were more tachycardic at baseline (579±10 vs 504±26 bpm, p=0.023, mixed level modelling), during the hypoxic challenge (721±7 vs 656±10 bpm, p<0.001) and during re-oxygenation (633±14 vs 560±26 bpm, p=0.049) compared to the pre-injection state. There was no difference in the change of HR during hypoxic challenge or recovery comparing pre- and post- Cre/GFP AVV injections.

$G\alpha_O$ flx/flx mice were also more hypertensive at baseline after the injections of Cre/GFP (152±7 vs 128±5 mmHg, p=0.025). There was a significant decrease in systolic BP on exposure to hypoxia (∆SBP -22mmHg, 95%CI -42 to -2 mmHg, p=0.034, Bonferroni) which was maintained during recovery post Cre/GFP AVV injection. As a result, systolic BP during (132±3 vs 129±5 mmHg, p=0.671) and after hypoxia (124±6 vs 126±6 mmHg, p= 0.796) were similar pre and post Cre/GFP AVV injections. Hypoxic ventilatory response was unaffected in conditions of $G\alpha_O$ deletion in the RVLM (Figures 4 and 6A, Table 1).

$G\alpha_O$ flx/flx mice responded to 6% CO_2 with a significant decrease in heart rate (∆HR -88 bpm, 95%CI -160 to -16 bpm, p=0.018), accompanied by an increase in the arterial BP (∆SBP 23 mmHg, 95% CI 5 to 41 mmHg, p=0.013). Hypercapnia also evoked stereotypic increases in minute ventilation. $G\alpha_O$ flx/flx mice displayed higher HR and systolic BP at baseline after acclimatisation to the chamber environment post Cre/GFP AVV injections (654±16 vs 587±23 bpm, p=0.012; 159±4 vs 136±6 mmHg, p=0.012). HR depression during hypercapnia was attenuated post Cre/GFP AVV injections (∆HR -21bpm, 95%CI -93 to 51 bpm, p=0.919), resulting in a consistently elevated HR throughout (3% CO2: 616±23 vs 539±28 bpm, p=0.049; 6% CO2: 633±19 vs 499±27 bpm, p=0.003). The elevation of systolic BP on exposure to 6% CO_2 was also attenuated post Cre/GFP AVV injections (∆SBP 11 95%CI -7 to 29 mmHg, p=0.248) resulting in a higher systolic BP compared to pre-injection (170±10 vs 159±4 mmHg, p=0.669). In summary, there is a significant difference in HR and systolic BP of mice at 6% CO_2 compared to baseline pre injection of Cre/GFP AVV which is lost with $G\alpha_O$ deletion post injection (Figures 5 and 6B, Table 2).

There were no differences in haemodynamic and respiratory parameters in $G\alpha_O$ flx/flx mice post GFP AVV injections at baseline and during hypoxic and hypercapnic challenges (Figures 4 and 5).

Haemodynamic profile and baroreflex sensitivity in conditions of $G\alpha_O$ deletion in the RVLM

$G\alpha_O$ flx/flx mice were next studied under urethane anaesthesia following injections of Cre/GFP AVV (n=5) and GFP AVV (n=5). In these conditions, $G\alpha_O$ flx/flx mice had significantly higher HR post Cre/GFP AVV injections compared to GFP AVV injections (629±3 v 598±5 bpm, p=0.002, *t* test) with no difference in systolic BP (111±2 vs 115±4 mmHg, p=0.074). This was associated with an increase in baroreflex gain (0.65±0.07 v 0.35±0.01 bpm $mmHg^{-1}$**,** p=0.012) (Figure 7 Table 3.

Ventricular excitability in conditions of $G\alpha_O$ deletion in the RVLM

Cre/GFP AVV (n=9) and GFP AVV (n=7) injected mice then underwent programmed electrical stimulation. The difference in resting heart rate was abolished following administration of atenolol with no effect on heart rate with additional administration of atropine. Cre/GFP AVV injected mice had significantly reduced $VERP_{750}$ compared to controls ($VERP_{750}$ 43±3 vs 55±4 ms, p=0.033, Mann-Whitney U) and this difference in $VERP_{750}$ was abolished by beta-adrenoceptor blockade with atenolol (Figure 8).

Discussion

$G\alpha_O$ is the major inhibitory heterotrimeric G-protein expressed in the brain and mediating inhibitory signalling by several neurotransmitters. In the present study we investigated whether $G\alpha_O$ mediated signalling is important in the central nervous mechanisms controlling cardiovascular activities focusing on the RVLM pre-sympathetic circuits. Our results show that mice with deletion of $G\alpha_O$ in the pre-sympathetic circuits of the brainstem (RVLM) display normal HR and arterial BP profile under resting conditions. However, when stressed in a novel environment or studied under general (urethane) anaesthesia, these mice show elevated HR and abnormal haemodynamic responses during systemic hypoxia and hypercapnia as well as increased baroreflex sensitivity. Pharmacological autonomic blockade using atenolol and atropine suggested that this phenotype is largely due to an increase in sympathetic tone. Finally, this increase in sympathetic tone to the heart was found to be associated with alterations in ventricular electrophysiology as evidenced from reduced VERP.

Deletion of $G\alpha_O$ proteins in the RVLM does not affect diurnal HR or BP under resting conditions

There were no significant differences in HR and BP profile after $G\alpha_O$ deletion in the pre-sympathetic area of the brainstem in conscious freely moving mice housed in standard conditions. This observation is in agreement with findings obtained in rats where permanent experimental perturbations within the C1 are likely to be compensated as previously reported (19; 33). These data suggest that impairment of RVLM function in controlling HR and BP can be fully compensated for in the awake and unstressed experimental animals.

Exaggerated heart rate responses to hypoxia and hypercapnia in mice with $G\alpha_O$ deletion in the RVLM

An increasing body of evidence is accumulating on the importance of the pre-sympathetic CNS circuits, and more specifically the RVLM, in mediating body responses to a variety of physiological and pathological stressors (9). Our data adds to this body of evidence of the key role played by the RVLM mechanisms under the conditions of environmental stress including hypoxia and hypercapnia. In addition, it would appear that inhibitory signalling in the brainstem mediated by $G\alpha_O$ proteins is an important mechanism restraining sympathetic activity. For example, the RVLM is activated by increased dorsomedial hypothalamic activity in response to psychological stressors (18; 22). This increased sympathetic activity is reversibly inhibited by selective serotonin-1A (5-HT1A) receptor agonist 8-OH-DPAT (11; 23; 25). 5-HT1A receptors are one of many GPCRs in the brainstem that signal via inhibitory $G\alpha_{i/o}$. In addition, GABA and enkephalins can tonically inhibit the RVLM potentially through G-protein coupled receptor pathways (2). GABA, 5-HT and adenosine are inhibitory neurotransmitters that have also all been shown to be released in the brainstem during hypoxia (31). Loss of inhibitory signalling mediated by $G\alpha_O$ could potentially explain the augmented HR response during the hypoxic challenge. The co-release of GABA with glutamate with similar temporal kinetics (31) suggests a role for GABA as a likely mediator of the restraining influence to the excitatory effects of glutamate during hypoxia. Indeed, there is evidence that GABA-ergic inhibitory mechanisms are important in modulating RVLM activity during hypoxia in rat neonatal brainstem preparations (3).

Increased sympathetic tone and its effect on ventricular excitability

Mice studied under urethane anaesthesia have previously been shown have reduced arterial pressure and increased HR compared to the conscious state (5; 30). Similar findings were obtained here with mice being hypotensive and generally more tachycardic. In general anaesthesia results in a reduction of vagal tone but urethane seems to lead to relative sparing compared to other anaesthetics (17). However, the RVLM does contain vagal preganglionic motoneurones (12). Sequential challenges with atenolol and atropine revealed low vagal tone and demonstrated that sympathetic activity indeed dominates heart rate

control in mice under urethane anaesthesia. This suggests that increased sympathetic outflow (rather than vagal withdrawal) is responsible for the increased heart rate and enhanced baroreflex sensitivity seen in mice with deletion of $G\alpha_O$ in the RVLM.

It is well known that the autonomic nervous system modulates cardiac excitability. Increase in sympathetic tone to the heart has been shown to reduce action potential duration with a corresponding increase in conduction velocity, resulting in a change in the restitution properties of action potential duration and dispersion of ventricular repolarisation and increased susceptibility to ventricular arrhythmia (7; 24). Our data adds to this body of evidence and demonstrates how alterations in central nervous mechanisms controlling cardiorespiratory activity can alter ventricular excitability.

G protein specificity in vivo

Parker et al has previously shown that $G\alpha_{i2}$ and $G\alpha_O$ are the most ubiquitous inhibitory G proteins in the RVLM (28). In keeping with this, our data suggest an important functional role for $G\alpha_O$. Although we cannot exclude a role for $G\alpha_{i2}$ as this was not studied directly with a conditional knockout of $G\alpha_{i2}$ in the brainstem. Our own previous studies show an effect on cardiac function in global $G\alpha_{i2}$ knockout mice though we have ascribed this largely to direct effects on cardiac tissue (43; 44). Other investigators have shown a potential role for $G\alpha_{i2}$ in the rat in mediating hypertensive responses (4; 42).

Limitations

The A1 and A5 cell groups and the vagal preganglionic neurones lie in close proximity to the RVLM in the ventral medullary brainstem region (37). Although great care was taken to target viral delivery to the RVLM area, given the non-specific nature of the CMV promoter, it is likely that some of the neurones in the neighbouring regions would have undergone Cre mediated deletion of $G\alpha_O$. However, given that the subsequent histological analysis demonstrated expression of GFP to be distributed among TH-immunoreactive

neurones in the RVLM region, the observed phenotype is likely to be due mainly to the loss of $G\alpha_O$-mediated signalling within the RVLM pre-sympathetic circuits.

The relative contributions of the sympathetic and parasympathetic limbs of the autonomic nervous system to the phenotype observed were assessed by pharmacological blockade. These are indirect measures of autonomic function. A more direct approach would involve direct recordings of efferent nerve activity such as of the renal sympathetic nerve (16) or other experimental paradigms such as in the working heart brainstem preparations (29).

The precise mechanism by which loss of $G\alpha_O$ at the RVLM results in alterations in autonomic tone remains unknown. We suggest that $G\alpha_O$ is important in mediating inhibitory influences on the RVLM with loss of this resulting in disinhibition and increased sympathetic outflow. $G\alpha_O$ coupled receptors can cause pre- or post-synaptic inhibition either by inhibiting calcium channels or activating G-protein gated K^+ channels respectively (6; 15). The specific neurotransmitter(s) and exact mechanism is a topic for further work in follow-up studies.

Conclusion

In summary, the data obtained in the present study suggest that $G\alpha_O$-mediated signalling within the pre-sympathetic circuits of the RVLM contributes to the autonomic control of the heart. $G\alpha_O$ deficiency in the RVLM is associated with exaggerated cardiovascular responses to stress, altered cardiovascular reflexes and ventricular excitability.

Conflicts of interest

The authors have no conflicts on interest to declare.

Funding

This research was supported by the Medical Resarch Council (MRC Clinical Research Training Fellowship to RA), British Heart Foundation (Ref: RG/14/4/30736),

Wellcome Trust (Wellcome Trust Senior Research Fellowship to AVG; Ref: 095064) and by the Intramural Research Program of the National Institutes of Health, National Institute of Environmental Health Sciences (Project Z01-ES-101643 to LB). This work was facilitated by the National Institute for Health Research Barts Cardiovascular Biomedical Research Unit.

Reference List

1. **Aziz Q, Thomas AM, Gomes J, Ang R, Sones WR, Li Y, Ng KE, Gee L and Tinker A**. The ATP-Sensitive Potassium Channel Subunit, Kir6.1, in Vascular Smooth Muscle Plays a Major Role in Blood Pressure Control. *Hypertension* 64: 523-529, 2014.

2. **Bowman BR, Kumar NN, Hassan SF, McMullan S and Goodchild AK**. Brain sources of inhibitory input to the rat rostral ventrolateral medulla. *J Comp Neurol* 521: 213-232, 2013.

3. **Boychuk CR, Woerman AL and Mendelowitz D**. Modulation of bulbospinal rostral ventral lateral medulla neurons by hypoxia/hypercapnia but not medullary respiratory activity. *Hypertension* 60: 1491-1497, 2012.

4. **Carmichael CY, Carmichael AC, Kuwabara JT, Cunningham JT and Wainford RD**. Impaired sodium-evoked paraventricular nucleus neuronal activation and blood pressure regulation in conscious Sprague-Dawley rats lacking central Galphai2 proteins. *Acta Physiol (Oxf)* 216: 314-329, 2016.

5. **Desai KH, Sato R, Schauble E, Barsh GS, Kobilka BK and Bernstein D**. Cardiovascular indexes in the mouse at rest and with exercise: new tools to study models of cardiac disease. *Am J Physiol* 272: H1053-H1061, 1997.

6. **Dolphin AC**. Mechanisms of modulation of voltage-dependent calcium channels by G proteins. *Journal of Physiology* 506: 3-11, 1998.

7. **Finlay MC, Lambiase PD, Ben-Simon R and Taggart P**. Effect of mental stress on dynamic electrophysiological properties of the endocardium and epicardium in humans. *Heart Rhythm* 13: 175-182, 2016.

8. **Gellen B, Fernandez-Velasco M, Briec F, Vinet L, LeQuang K, Rouet-Benzineb P, Benitah JP, Pezet M, Palais G, Pellegrin N, Zhang A, Perrier R, Escoubet B, Marniquet X, Richard S, Jaisser F, Gomez AM, Charpentier F and Mercadier JJ**. Conditional FKBP12.6 overexpression in mouse cardiac myocytes prevents triggered ventricular tachycardia through specific alterations in excitation-contraction coupling. *Circulation* 117: 1778-1786, 2008.

9. **Guyenet PG, Stornetta RL, Bochorishvili G, Depuy SD, Burke PG and Abbott SB**. C1 neurons: the body's EMTs. *Am J Physiol Regul Integr Comp Physiol* 305: R187-R204, 2013.

10. **Head GA and McCarty R**. Vagal and sympathetic components of the heart rate range and gain of the baroreceptor-heart rate reflex in conscious rats. *Journal of the Autonomic Nervous System* 21: 203-213, 2002.

11. **Horiuchi J, McDowall LM and Dampney RA**. Role of 5-HT(1A) receptors in the lower brainstem on the cardiovascular response to dorsomedial hypothalamus activation. *Auton Neurosci* 142: 71-76, 2008.

12. **Izzo PN, Deuchars J and Spyer KM**. Localization of cardiac vagal preganglionic motoneurones in the rat: immunocytochemical evidence of synaptic inputs containing 5-hydroxytryptamine. *J Comp Neurol* 327: 572-583, 1993.

13. **LaVallie ER, Chockalingam PS, Collins-Racie LA, Freeman BA, Keohan CC, Leitges M, Dorner AJ, Morris EA, Majumdar MK and Arai M**. Protein kinase Czeta is up-regulated in osteoarthritic cartilage and is required for activation of NF-kappaB by tumor necrosis factor and interleukin-1 in articular chondrocytes. *J Biol Chem* 281: 24124-24137, 2006.

14. **Lopez M, Lage R, Saha AK, Perez-Tilve D, Vazquez MJ, Varela L, Sangiao-Alvarellos S, Tovar S, Raghay K, Rodriguez-Cuenca S, Deoliveira RM, Castaneda T, Datta R, Dong JZ, Culler M, Sleeman MW, Alvarez CV, Gallego R, Lelliott CJ, Carling D, Tschop MH, Dieguez C and Vidal-Puig A**. Hypothalamic fatty acid metabolism mediates the orexigenic action of ghrelin. *Cell Metab* 7: 389-399, 2008.

15. **Luscher C and Slesinger PA**. Emerging roles for G protein-gated inwardly rectifying potassium (GIRK) channels in health and disease. *Nat Rev Neurosci* 11: 301-315, 2010.

16. **Ma X, Abboud FM and Chapleau MW**. Analysis of afferent, central, and efferent components of the baroreceptor reflex in mice. *Am J Physiol Regul Integr Comp Physiol* 283: R1033-R1040, 2002.

17. **Machhada A, Ang R, Ackland GL, Ninkina N, Buchman VL, Lythgoe MF, Trapp S, Tinker A, Marina N and Gourine AV**. Control of ventricular excitability by neurons of the dorsal motor nucleus of the vagus nerve. *Heart Rhythm* 12: 2285-2293, 2015.

18. **Madden CJ and Morrison SF**. Excitatory amino acid receptors in the dorsomedial hypothalamus mediate prostaglandin-evoked thermogenesis in brown adipose tissue. *Am J Physiol Regul Integr Comp Physiol* 286: R320-R325, 2004.

19. **Madden CJ and Sved AF**. Cardiovascular regulation after destruction of the C1 cell group of the rostral ventrolateral medulla in rats. *Am J Physiol Heart Circ Physiol* 285: H2734-H2748, 2003.

20. **Marina N, Abdala AP, Korsak A, Simms AE, Allen AM, Paton JF and Gourine AV**. Control of sympathetic vasomotor tone by catecholaminergic C1 neurones of the rostral ventrolateral medulla oblongata. *Cardiovasc Res* 91: 703-710, 2011.

21. **Marina N, Ang R, Machhada A, Kasymov V, Karagiannis A, Hosford PS, Mosienko V, Teschemacher AG, Vihko P, Paton JF, Kasparov S and Gourine AV**. Brainstem hypoxia contributes to the development of hypertension in the spontaneously hypertensive rat. *Hypertension* 65: 775-783, 2015.

22. **Nalivaiko E and Blessing WW**. Raphe region mediates changes in cutaneous vascular tone elicited by stimulation of amygdala and hypothalamus in rabbits. *Brain Res* 891: 130-137, 2001.

23. **Nalivaiko E, Ootsuka Y and Blessing WW**. Activation of 5-HT1A receptors in the medullary raphe reduces cardiovascular changes elicited by acute psychological and inflammatory stresses in rabbits. *Am J Physiol Regul Integr Comp Physiol* 289: R596-R604, 2005.

24. **Ng GA, Mantravadi R, Walker WH, Ortin WG, Choi BR, de GW and Salama G**. Sympathetic nerve stimulation produces spatial heterogeneities of action potential restitution. *Heart Rhythm* 6: 696-706, 2009.

25. **Ngampramuan S, Baumert M, Beig MI, Kotchabhakdi N and Nalivaiko E**. Activation of 5-HT(1A) receptors attenuates tachycardia induced by restraint stress in rats. *Am J Physiol Regul Integr Comp Physiol* 294: R132-R141, 2008.

26. **Nolan J, Batin PD, Andrews R, Lindsay SJ, Brooksby P, Mullen M, Baig W, Flapan AD, Cowley A, Prescott RJ, Neilson JM and Fox KA**. Prospective study of

heart rate variability and mortality in chronic heart failure: results of the United Kingdom heart failure evaluation and assessment of risk trial (UK-heart). *Circulation* 98: 1510-1516, 1998.

27. **Onodera M, Kuwaki T, Kumada M and Masuda Y**. Determination of ventilatory volume in mice by whole body plethysmography. *Jpn J Physiol* 47: 317-326, 1997.

28. **Parker LM, Tallapragada VJ, Kumar NN and Goodchild AK**. Distribution and localisation of Galpha proteins in the rostral ventrolateral medulla of normotensive and hypertensive rats: focus on catecholaminergic neurons. *Neuroscience* 218: 20-34, 2012.

29. **Paton JF**. A working heart-brainstem preparation of the mouse. *J Neurosci Methods* 65: 63-68, 1996.

30. **Paton JF and Butcher JW**. Cardiorespiratory reflexes in mice. *J Auton Nerv Syst* 68: 115-124, 1998.

31. **Richter DW, Schmidt-Garcon P, Pierrefiche O, Bischoff AM and Lalley PM**. Neurotransmitters and neuromodulators controlling the hypoxic respiratory response in anaesthetized cats. *J Physiol* 514 (Pt 2): 567-578, 1999.

32. **Rong W, Gourine AV, Cockayne DA, Xiang Z, Ford AP, Spyer KM and Burnstock G**. Pivotal role of nucleotide P2X2 receptor subunit of the ATP-gated ion channel mediating ventilatory responses to hypoxia. *J Neurosci* 23: 11315-11321, 2003.

33. **Schreihofer AM, Stornetta RL and Guyenet PG**. Regulation of sympathetic tone and arterial pressure by rostral ventrolateral medulla after depletion of C1 cells in rat. *J Physiol* 529 Pt 1: 221-236, 2000.

34. **Sebastian S, Ang R, Abramowitz J, Weinstein LS, Chen M, Ludwig A, Birnbaumer L and Tinker A**. The in-vivo regulation of heart rate in the murine sinoatrial node by stimulatory and inhibitory heterotrimeric G-proteins. *Am J Physiol Regul Integr Comp Physiol* 305: 435-442, 2013.

35. **Spyer KM**. Annual review prize lecture. Central nervous mechanisms contributing to cardiovascular control. *J Physiol* 474: 1-19, 1994.

36. **Sternweis PC and Robishaw JD**. Isolation of two proteins with high affinity for guanine nucleotides from membranes of bovine brain. *J Biol Chem* 259: 13806-13813, 1984.

37. **Strack AM, Sawyer WB, Platt KB and Loewy AD**. CNS cell groups regulating the sympathetic outflow to adrenal gland as revealed by transneuronal cell body labeling with pseudorabies virus. *Brain Res* 491: 274-296, 1989.

38. **Trapp S, Tucker SJ and Gourine AV**. Respiratory responses to hypercapnia and hypoxia in mice with genetic ablation of Kir5.1 (Kcnj16). *Exp Physiol* 96: 451-459, 2011.

39. **Ustyugova IV, Zhi L, Abramowitz J, Birnbaumer L and Wu MX**. IEX-1 deficiency protects against colonic cancer. *Mol Cancer Res* 10: 760-767, 2012.

40. **Vaseghi M, Gima J, Kanaan C, Ajijola OA, Marmureanu A, Mahajan A and Shivkumar K**. Cardiac sympathetic denervation in patients with refractory ventricular arrhythmias or electrical storm: intermediate and long-term follow-up. *Heart Rhythm* 11: 360-366, 2014.

41. **Verrier RL and Antzelevitch C**. Autonomic aspects of arrhythmogenesis: the enduring and the new. *Curr Opin Cardiol* 19: 2-11, 2004.

42. **Wainford RD, Carmichael CY, Pascale CL and Kuwabara JT**. Galphai2-protein-mediated signal transduction: central nervous system molecular mechanism countering the development of sodium-dependent hypertension. *Hypertension* 65: 178-186, 2015.

43. **Zuberi Z, Birnbaumer L and Tinker A**. The role of inhibitory heterotrimeric G-proteins in the control of in-vivo heart rate dynamics. *Am J Physiol Regul Integr Comp Physiol* 295: R1822-R1830, 2008.

44. **Zuberi Z, Nobles M, Sebastian S, Dyson A, Shiang Y, Breckenridge RA, Birnbaumer L and Tinker A**. Absence of the inhibitory G-protein, $G\alpha_{i2}$, predisposes to ventricular cardiac arrhythmia. *Circ Arrhythm Electrophysiol* 3: 391-400, 2010.

Figure Legends

Figure 1. Experimental protocol for conscious experiments.

Figure showing timeline of conscious experimental protocols. AVV injection to the brainstem is performed at Day 0.

Figure 2. GFP expression in TH-positive neurones in the brainstem.

(A), Green fluorescent protein (GFP) expression in the C1 region of the RVLM (TH, tyrosine hydroxylase). Bottom image is a high magnification micrograph showing two TH-positive neurones expressing GFP. **(B),** Schematic drawing of the mouse brainstem in a series of coronal projections illustrating the representative extent of GFP expression in relation to the anatomic location of the RVLM presympathetic circuits. Numbers indicate distance from Bregma. GFP expression was highest in the ventrolateral medullary regions located at −6.80 mm from Bregma**.**

Figure 3. 24 hour haemodynamic profile in conscious freely moving mice under normal housing conditions.

(A) Heart rate (HR) and systolic blood pressure (SBP) of $G\alpha_O$ flx/flx mice pre- and post- GFP and Cre/GFP AVV injections into the brainstem measured using biotelemetry over a 24 hour period. **(B)** Summary data of mean systolic arterial BP recorded (top) and HR (bottom) in $G\alpha_O$ flx/flx mice pre and post GFP AVV (GFP) and Cre/GFP AVV (Cre) injections into the brainstem. Data expressed as mean ± SEM, n=6 in all groups.

Figure 4. Haemodynamic and respiratory responses to hypoxia.

(A) Representative heart rate (HR), arterial blood pressure (BP), respiratory rate (RR) and respiratory pressure (RESP) tracings of a $G\alpha_O$ flx/flx mouse post GFP AVV (left panel) and Cre/GFP AVV (right panel) injections respectively subjected to normoxia, hypoxia (10%

inspired O_2) and a recovery period. **(B)** HR, SBP, RR and minute volume ventilation (MV) pre and post control GFP AVV (n=4, left panel) and Cre/GFP AVV (n=6, right panel) injections. Individual data and mean ± SEM are shown.

* p<0.05, ***p<0.001. a.u.: arbitrary units.

Figure 5. Haemodynamic and respiratory responses to hypercapnia.

(A) Representative heart rate (HR) and arterial blood pressure (BP), respiratory rate (RR) and respiratory pressure (RESP) tracings of a $G\alpha_O$ flx/flx mouse post GFP AVV (left panel) and Cre/GFP AVV (right panel) injections respectively subjected to normoxia, 3% inspired CO_2 and 6% inspired CO_2. **(B)** HR, SBP, RR and minute volume ventilation (MV) pre and post control GFP AVV (n=4, left panel) and Cre/GFP AVV (n=6, right panel) injections. Individual data and mean ± SEM are shown.

* p<0.05, **p<0.01. abu: arbitrary units.

Figure 6 Changes in HR and systolic BP in response to hypoxia and hypercapnia

Plots of the mean difference and 95% CI of heart rate (HR) and systolic BP (SBP) in $G\alpha_O$ flx/flx mice in response to **(A)** hypoxia and **(B)** hypercapnia.

Figure 7. Baroreflex response under urethane anaesthesia.

(A) Representative tracings of arterial blood pressure (BP) and heart rate (HR) of a $G\alpha_O$ flx/flx mouse post Cre/GFP injection given alternating boluses of phenylephrine (PE) and sodium nitroprusside (SNP). **(B)** An example of a best-fit HR and systolic BP baroreflex curve constructed from data points obtained. **(C)** Mean baroreflex curves (bold lines) for mice injected with Cre/GFP and GFP AVV (n=5 in each group). Bold points represent mean HR 50 and SBP 50 for each group.

Figure 8. Effect of autonomic blockade on heart rate and ventricular excitability.

(A) Representative in vivo cardiac electrophysiology data produced by programmed electrical stimulation showing an example of right ventricular effective refractory period (VERP) in $G\alpha_O$ flx/flx mouse injected with Cre/GFP AVV compared to control GFP AVV with lengthening of VERP on administration of Atenolol. (B) Representative example of ventricular tachycardia (VT) induced by burst pacing in a $G\alpha_O$ flx/flx mouse injected with Cre/GFP AVV on the right panel as evidenced by dissociation of ventricular (V) compared to atrial (A) signals. Left panel shows an example of no VT inducible in mice injected with GFP AVV. (C) Comparison of HR and (D) $VERP_{750}$ between $G\alpha_O$ flx/flx mice post- GFP (GFP, n=7) and Cre/GFP (Cre, n=9) AVV injections at baseline and after administration of atenolol 1mg/kg ip +/- atropine 1mg/kg ip. Data expressed as mean ± SEM. * $p<0.05$, *** $p<0.001$.

ECG: surface ECG; Intracardiac: intracardiac electrograms; Stim: pacing stimulus. V: Ventricular activity; A: Atrial activity.

		Baseline		10% O_2		Recovery	
		GFP (n=4)	Cre (n=6)	GFP (n=4)	Cre (n=6)	GFP (n=4)	Cre (n=6)
Heart rate (BPM)	Pre	527±13	504±26	665±11	656±10	559±20	560±26
	Post	495±28	* **579±10**	665±16	*** **721±7**	524±30	* **633±14**
Systolic blood pressure (mmHg)	Pre	129±6	128±5	124±3	132±3	129±4	124±6
	Post	135±5	* **152±7**	126±6	129±5	128±7	126±6
Diastolic blood pressure (mmHg)	Pre	62±7	68±6	62±5	69±5	62±6	66±6
	Post	68±6	* **81±8**	65±6	64±4	63±5	61±7
Respiratory rate (min^{-1})	Pre	185±5	199±7	280±6	263±7	145±11	167±10
	Post	191±3	199±8	271±3	266±6	153±9	155±9
Minute volume (au g^{-1} min^{-1})	Pre	1.0±0.1	1.0±0.1	3.4±0.1	3.3±0.2	1.1±0.1	1.2±0.1
	Post	1.0±0.1	1.1±0.1	3.2±0.2	3.5±0.2	1.1±0.1	1.4±0.1

Table 1 Summary data of hypoxia-induced changes in haemodynamic and respiratory variables recorded in Control (n=4) and $G\alpha_o$ floxed brainstem Cre mice (n=6) pre- and post- viral injections.

Data are expressed as means ± SEM. Values highlighted in bold are significantly different when compared to pre-injection values. ** p<0.05, *** P<0.001*

		Baseline		3% CO_2		6% CO_2	
		GFP (n=4)	Cre (n=6)	GFP (n=4)	Cre (n=6)	GFP (n=4)	Cre (n=6)
Heart rate (BPM)	Pre	521±41	587±23	518±22	539±28	518±22	499±27
	Post	507±24	* **654±16**	474±26	* **616±23**	474±26	** **633±19**
Systolic blood pressure (mmHg)	Pre	135±9	136±6	155±14	152±9	169±8	164±9
	Post	137±8	* **159±4**	160±9	163±9	173±10	170±10
Diastolic blood pressure (mmHg)	Pre	65±8	67±7	65±10	69±8	66±7	63±8
	Post	64±7	* **83±6**	63±8	66±9	64±8	62±9
Respiratory rate (min^{-1})	Pre	198±4	196±6	218±4	223±8	260±12	269±14
	Post	202±7	201±5	229±12	221±11	265±10	307±23
Minute volume (au g^{-1} min^{-1})	Pre	1.0±0.1	0.9±0.1	1.9±0.2	1.7±0.1	2.9±0.1	3.0±0.4
	Post	0.8±0.2	1.0±0.1	1.7±0.3	1.9±0.3	2.9±0.3	4.7±0.9

Table 2 Summary data of hypercapnia-induced changes in haemodynamic and respiratory variables recorded in Control (n=4) and $G\alpha_O$ floxed brainstem Cre mice (n=6) pre- and post- viral injections.

Data are expressed as means ± SEM. Values highlighted in bold are significantly different when compared to pre-injection values. ** p<0.05, ** P<0.01*

	Cre (n=5)	GFP control (n=5)	P value
HR min (bpm)	**604±2**	**575±9 ***	**0.028**
HR 50 (bpm)	**629±3**	**598±5****	**0.002**
HR max (bpm)	**654±6**	**620±4 ***	**0.017**
HR range (bpm)	50±6	48±7	0.451
SBP min (mmHg)	50±4	43±6	0.399
SBP 50 (mmHg)	115±4	101±2	0.074
SBP max (mmHg)	155±5	153±5	0.850
BP range (mmHg)	114±6	107±2	0.325
BR gain (bpm $mmHg^{-1}$)	**0.65±0.07**	**0.35±0.01***	**0.012**

Table 3 Summary data of parameters derived from baroreflex curve for mice with conditional deletion of $G\alpha_o$ in the RVLM compared to controls

Data are expressed as means ± SEM. Values highlighted in bold are significantly different when compared to controls. * *P<0.05*, ** *P<0.01*

Figure 1

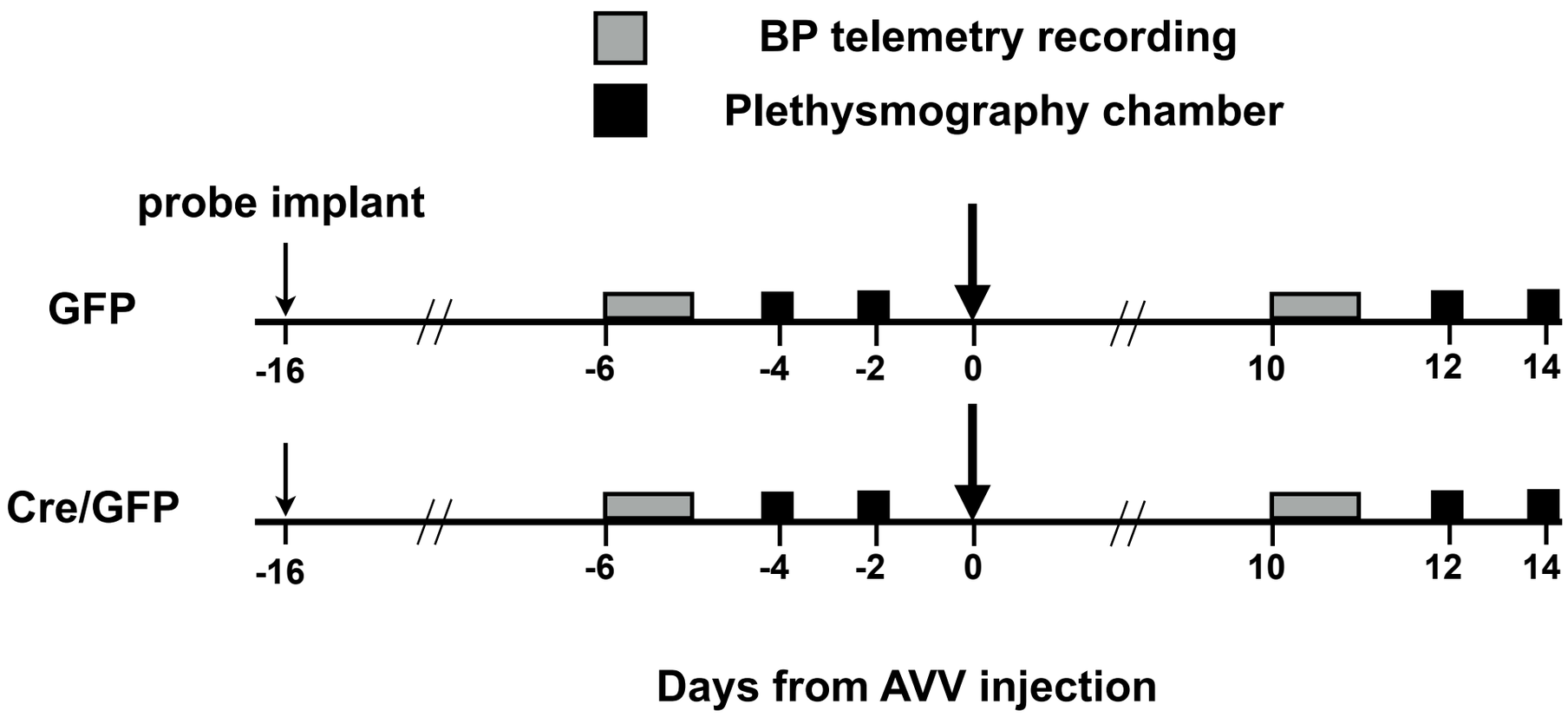
BP telemetry recording
Plethysmography chamber
probe implant
GFP
-16
-6
-4
-2
0
10
12
14
Cre/GFP
-16
-6
-4
-2
0
10
12
14
Days from AVV injection

Figure 2

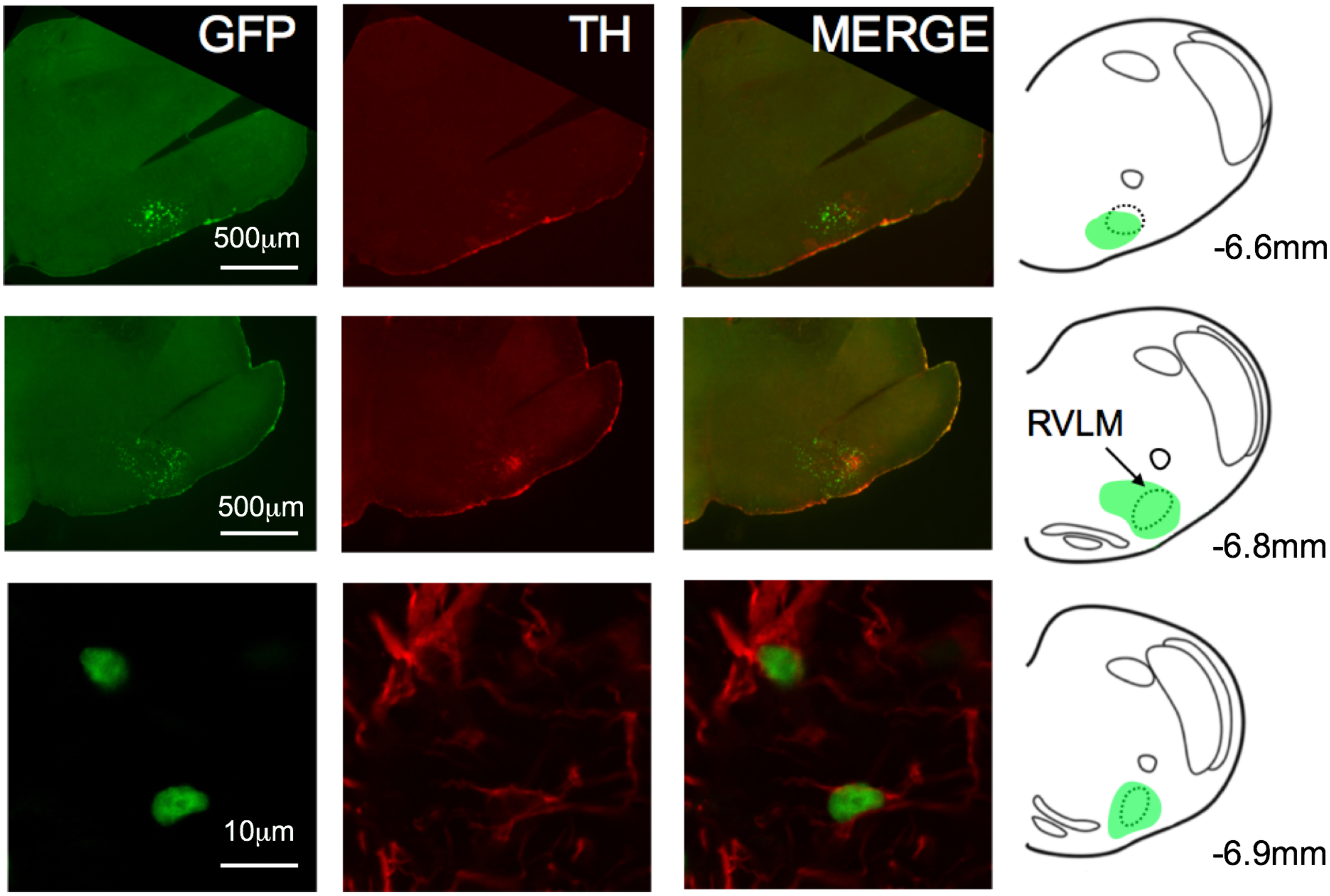

Figure 3

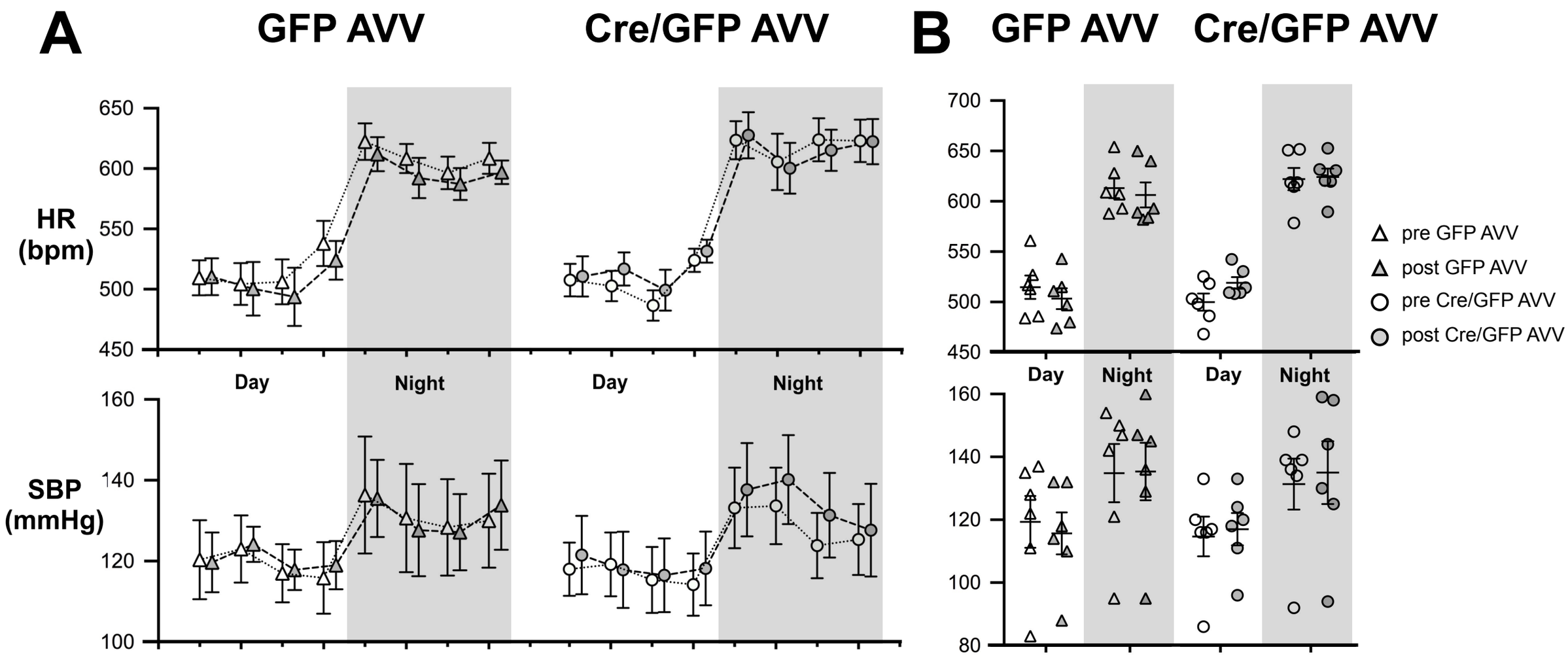
A
GFP AVV
Cre/GFP AVV
HR (bpm)
650
600
550
500
450
Day
Night
Day
Night
SBP (mmHg)
160
140
120
100
B
GFP AVV
Cre/GFP AVV
700
650
600
550
500
450
160
140
120
100
80
Day
Night
Day
Night
pre GFP AVV
post GFP AVV
pre Cre/GFP AVV
post Cre/GFP AVV

Figure 4

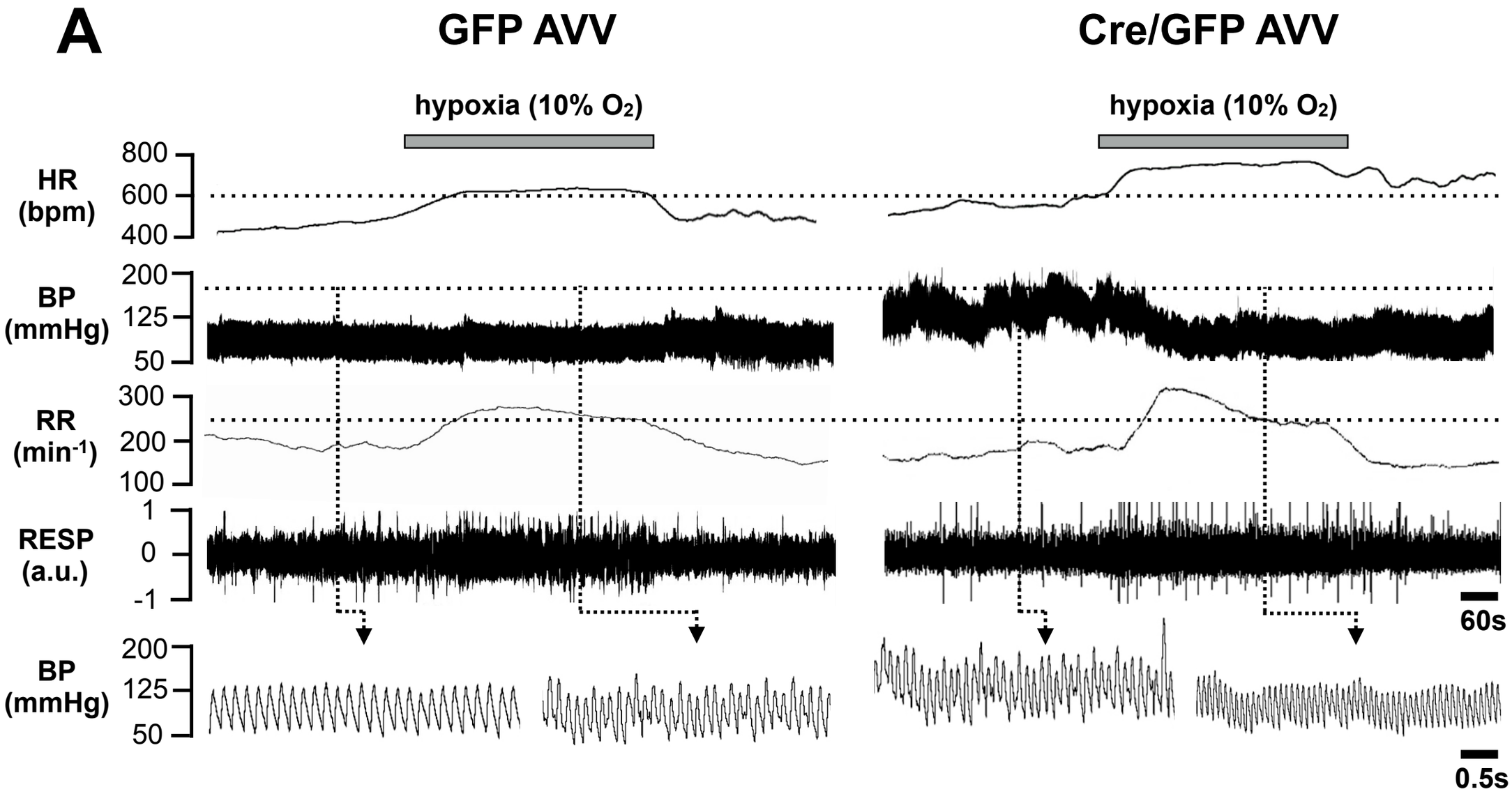
A
GFP AVV
Cre/GFP AVV
hypoxia (10% O2)
hypoxia (10% O2)
HR (bpm)
800
600
400
BP (mmHg)
200
125
50
RR (min-1)
300
200
100
RESP (a.u.)
1
0
-1
BP (mmHg)
200
125
50
60s
0.5s

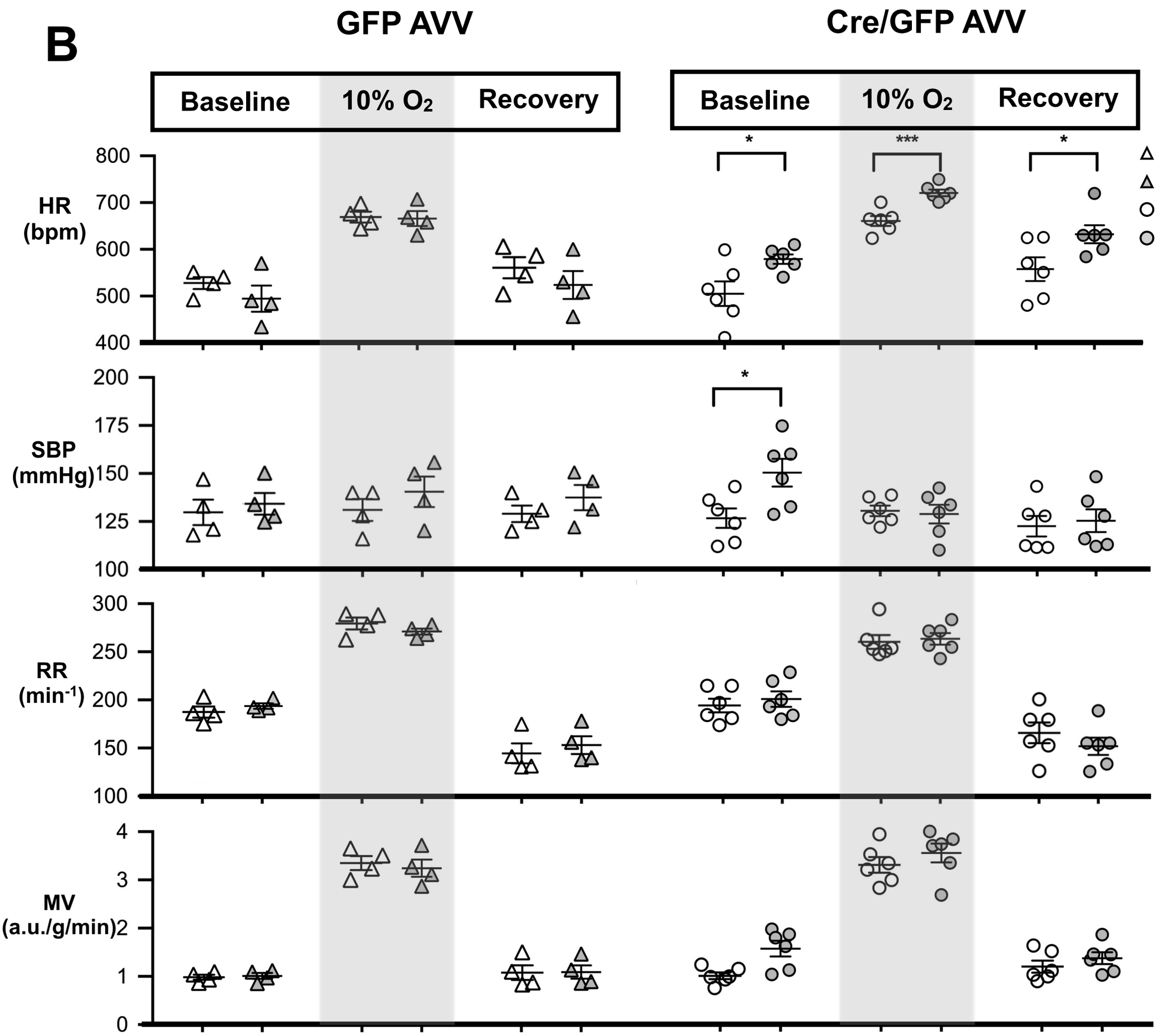
B
GFP AVV
Cre/GFP AVV
Baseline
10% O2
Recovery
Baseline
10% O2
Recovery
*
***
*
pre GFP AVV
post GFP AVV
pre Cre/GFP AVV
post Cre/GFP AVV
HR (bpm)
800
700
600
500
400
SBP (mmHg)
200
175
150
125
100
*
RR (min-1)
300
250
200
150
100
MV (a.u./g/min)
4
3
2
1
0

Figure 5

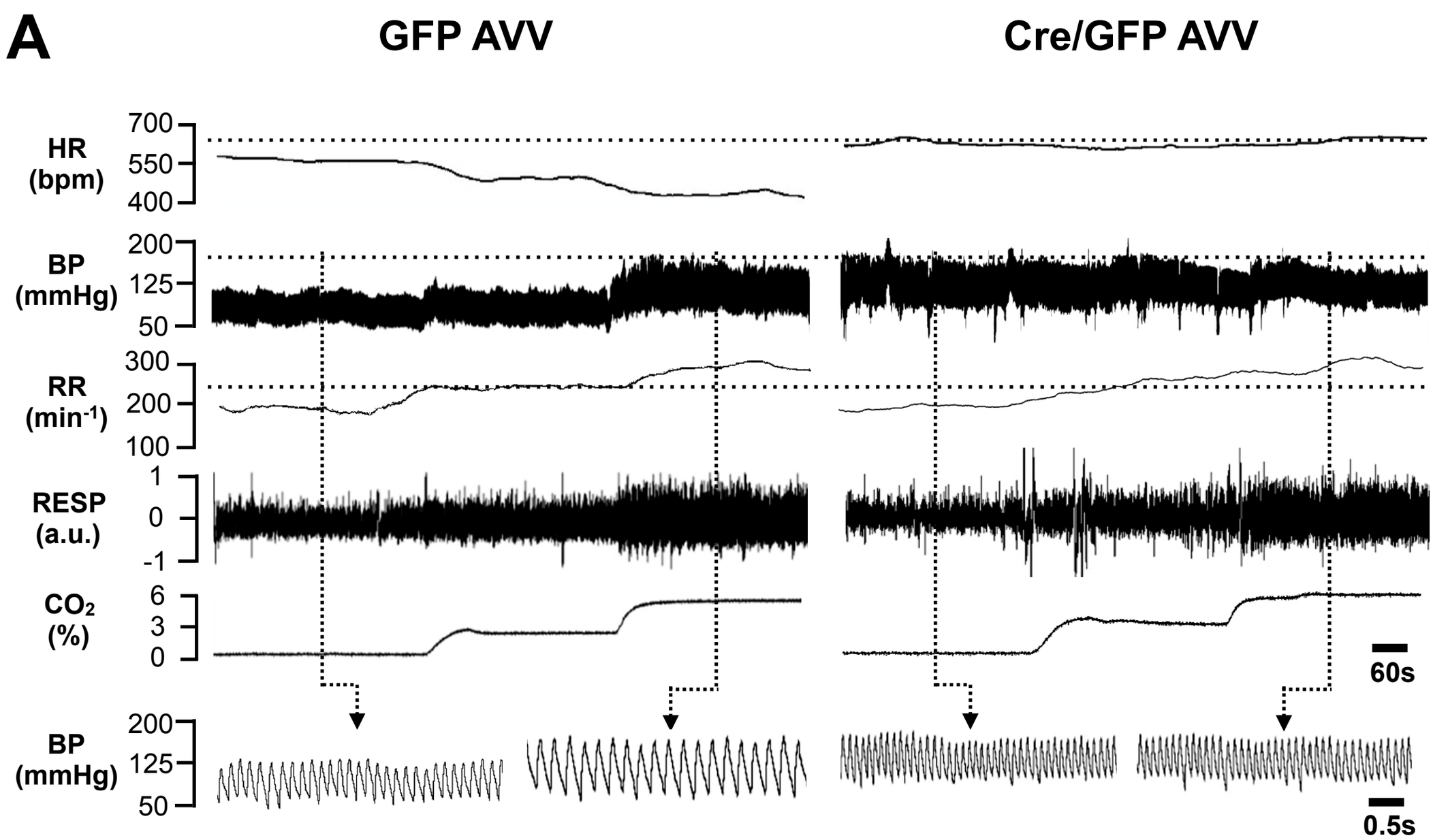
A
GFP AVV
Cre/GFP AVV
HR (bpm)
700
550
400
BP (mmHg)
200
125
50
RR (min-1)
300
200
100
RESP (a.u.)
1
0
-1
CO2 (%)
6
3
0
60s
0.5s

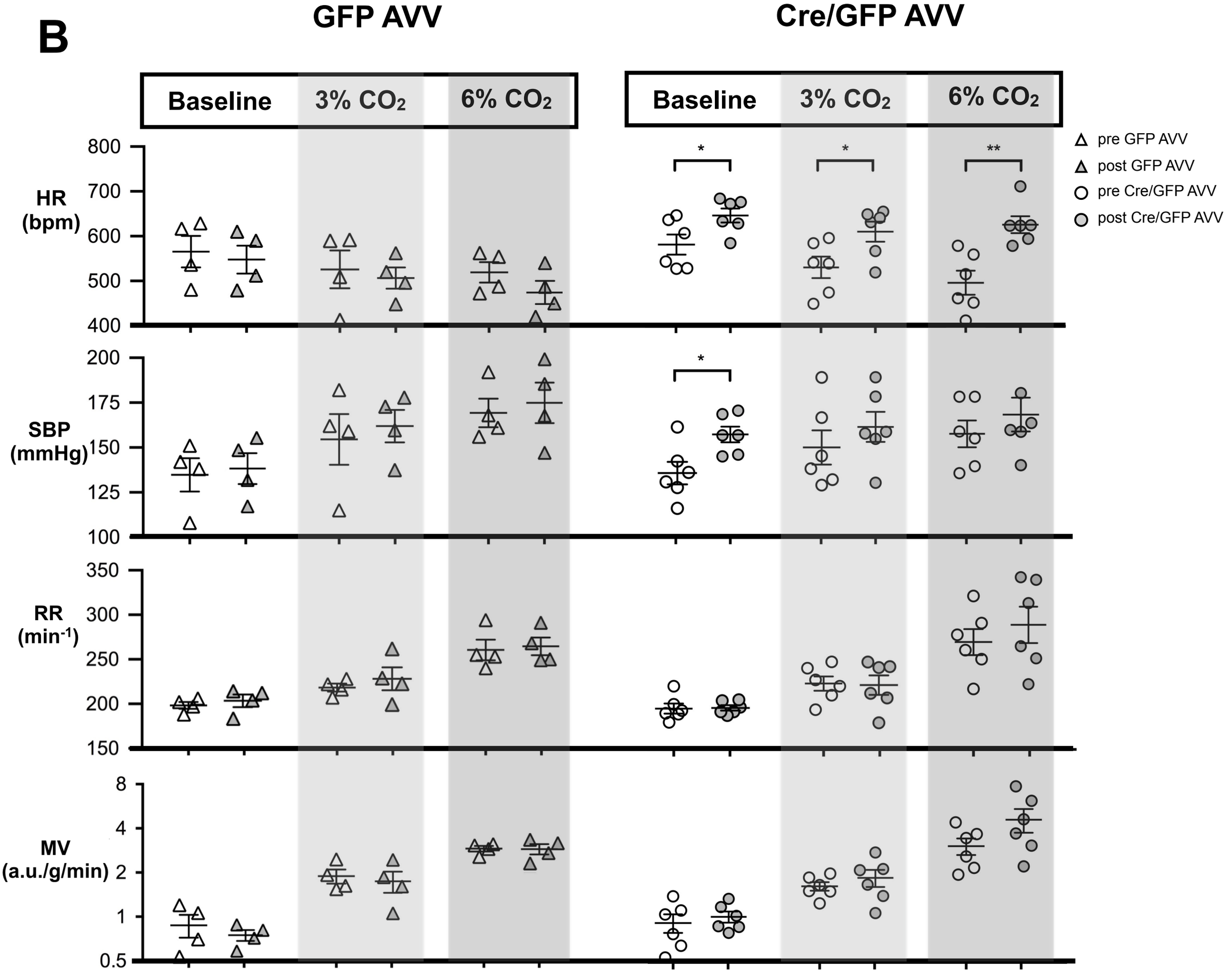
B
GFP AVV
Cre/GFP AVV
Baseline
3% CO2
6% CO2
pre GFP AVV
post GFP AVV
pre Cre/GFP AVV
post Cre/GFP AVV
HR (bpm)
800
700
600
500
400
SBP (mmHg)
200
175
150
125
100
RR (min-1)
350
300
250
200
150
MV (a.u./g/min)
8
4
2
1
0.5
*
*
**
*

Figure 6

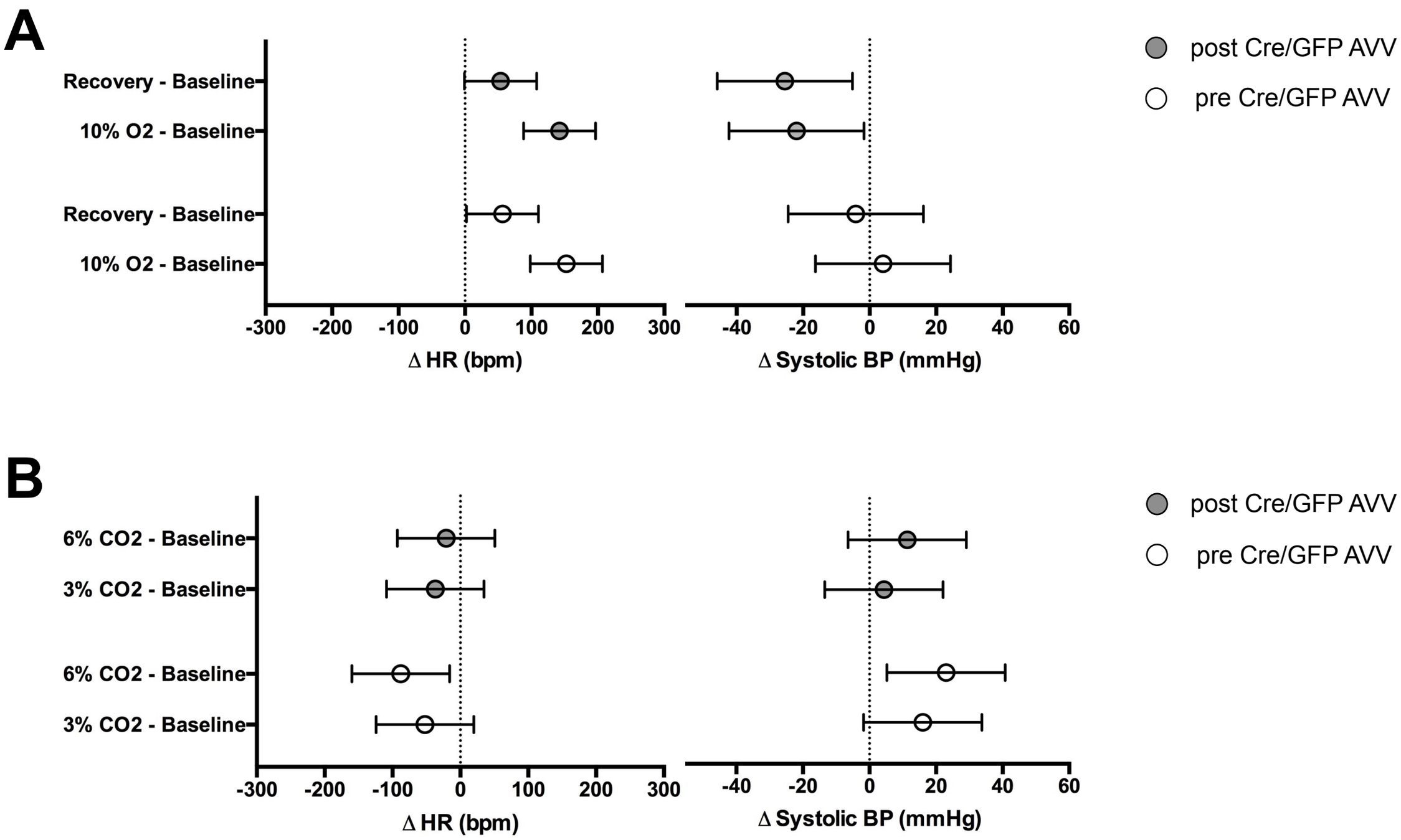
A
Recovery - Baseline
10% O2 - Baseline
Recovery - Baseline
10% O2 - Baseline
-300
-200
-100
0
100
200
300
Δ HR (bpm)
-40
-20
0
20
40
60
Δ Systolic BP (mmHg)
post Cre/GFP AVV
pre Cre/GFP AVV
B
6% CO2 - Baseline
3% CO2 - Baseline
6% CO2 - Baseline
3% CO2 - Baseline
-300
-200
-100
0
100
200
300
Δ HR (bpm)
-40
-20
0
20
40
60
Δ Systolic BP (mmHg)
post Cre/GFP AVV
pre Cre/GFP AVV

Figure 7

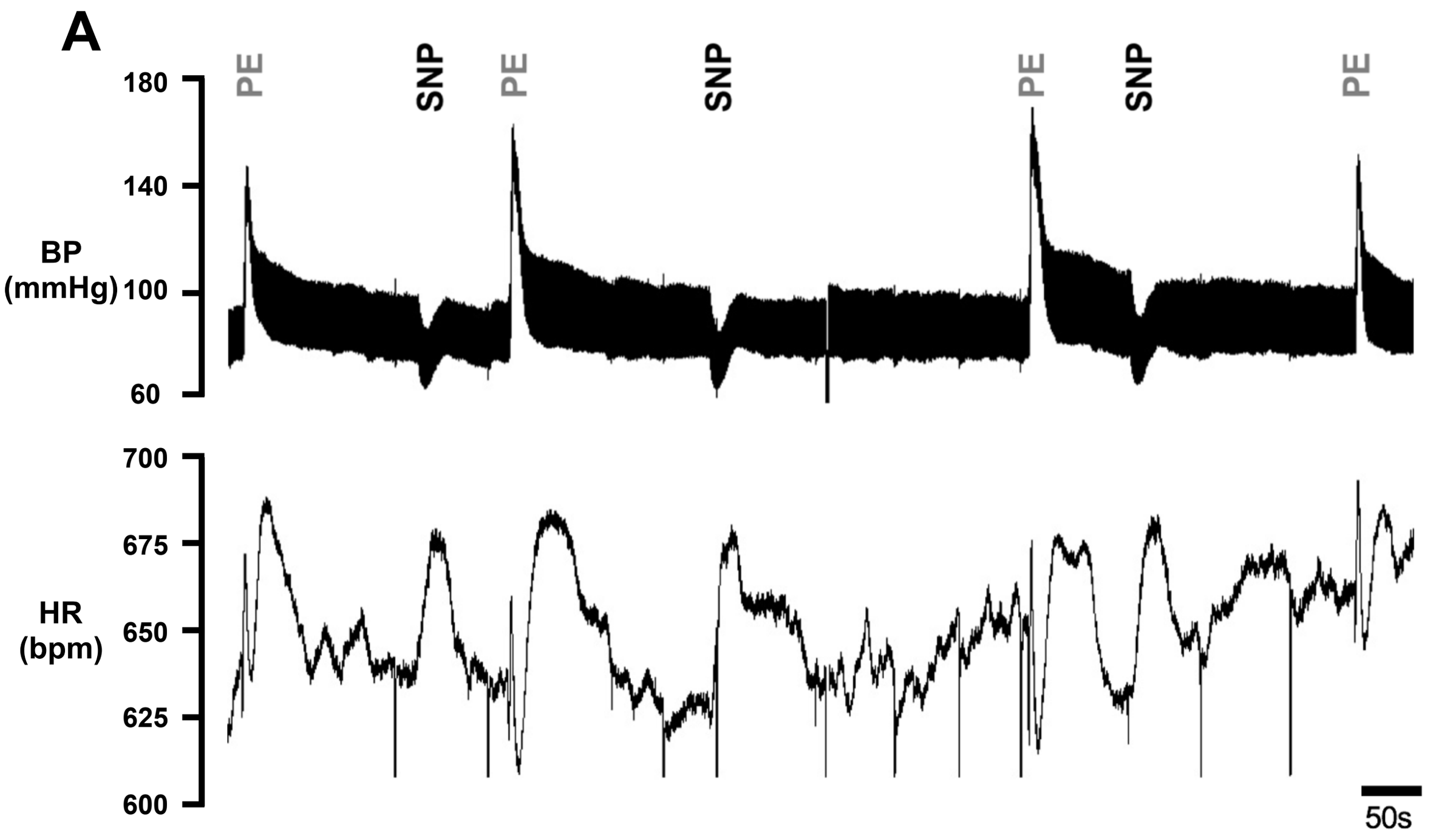
A
PE
SNP
PE
SNP
PE
SNP
PE
180
140
BP
(mmHg)
100
60
700
675
HR
(bpm)
650
625
600
50s

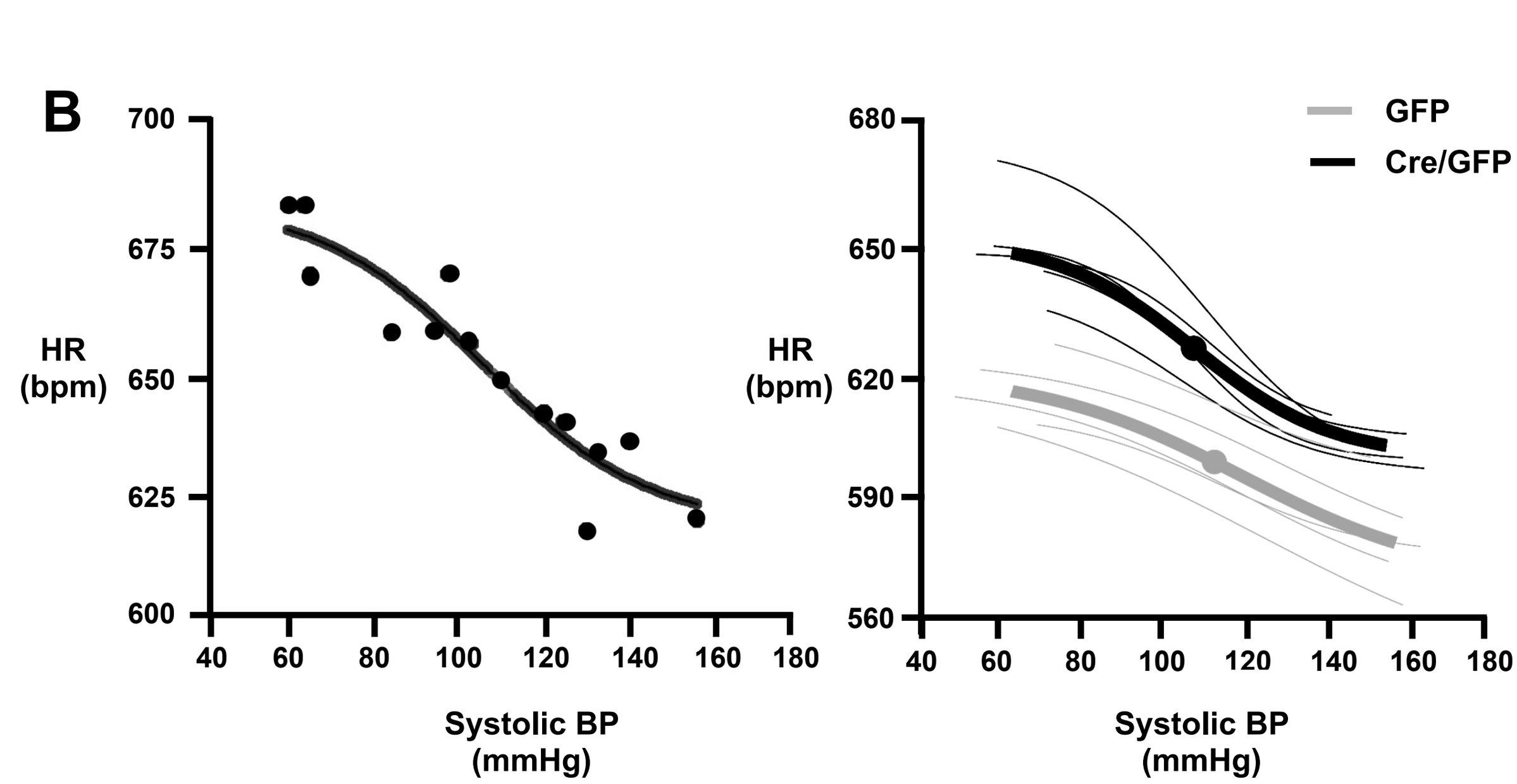
B
700
675
HR
(bpm)
650
625
600
40
60
80
100
120
140
160
180
Systolic BP
(mmHg)
680
650
620
590
560
HR
(bpm)
GFP
Cre/GFP
40
60
80
100
120
140
160
180
Systolic BP
(mmHg)

Figure 8

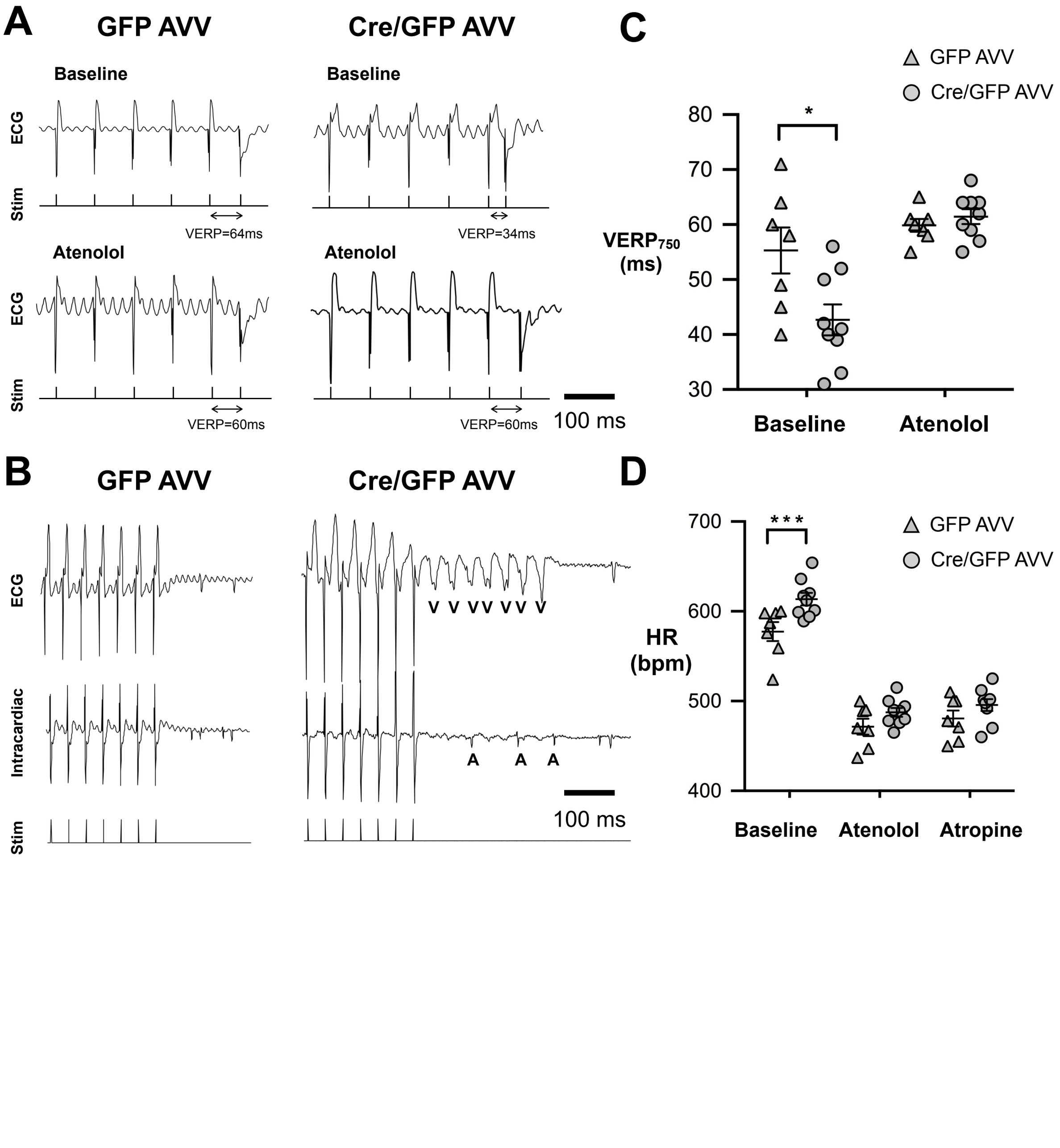
A
GFP AVV
Cre/GFP AVV
Baseline
ECG
Stim
VERP=64ms
VERP=34ms
Atenolol
VERP=60ms
100 ms
C
GFP AVV
Cre/GFP AVV
VERP750 (ms)
80
70
60
50
40
30
*
Baseline
Atenolol
B
GFP AVV
Cre/GFP AVV
ECG
Intracardiac
Stim
V V VV VV V
A A A
100 ms
D
HR (bpm)
700
600
500
400
***
Baseline
Atenolol
Atropine